OSAL-ND: Open-set Active Learning for Nucleus Detection

Jiao Tang[1], Yagao Yue[1], Peng Wan[1], Mingliang Wang[2], Daoqiang Zhang (✉)[1], and Wei Shao (✉)[1]

[1] College of Artificial Intelligence, Nanjing University of Aeronautics and Astronautics, Key Laboratory of Brain-Machine Intelligence Technology, Ministry of Education, Nanjing 211106, China
dqzhang@nuaa.edu.cn, shaowei20022005@nuaa.edu.cn
[2] School of Computer Science, Nanjing University of Information Science and Technology

Abstract. The recent advance of deep learning has shown promising power for nucleus detection that plays an important role in histopathological examination. However, such accurate and reliable deep learning models need enough labeled data for training, which makes active learning (AL) an attractive learning paradigm for reducing the annotation efforts by pathologists. In open-set environments, AL encounters the challenge that the unlabeled data usually contains non-target samples from the unknown classes, resulting in the failure of most AL methods. Although AL has been explored in many open-set classification tasks, research on AL for nucleus detection in the open-set environment remains unexplored. To address the above issues, we propose a two-stage AL framework designed for nucleus detection in an open-set environment (i.e., OSAL-ND). In the first stage, we propose a prototype-based query strategy based on the auxiliary detector to select a candidate set from known classes as pure as possible. In the second stage, we further query the most uncertain samples from the candidate set for the nucleus detection task relying on the target detector. We evaluate the performance of our method on the NuCLS dataset, and the experimental results indicate that our method can not only improve the selection quality on the known classes, but also achieve higher detection accuracy with lower annotation burden in comparison with the existing studies.

Keywords: Nucleus Detection · Active Learning · Open-Set Detection · Histopathological Images.

1 Introduction

H&E stained histopathological image is a routine and most common protocol used by pathologists for estimating the aggressiveness of human cancer [5,19]. Given the digital histopathological images, accurate detection of their involved nuclei is a crucial step for tumor assessment (staging, grading, etc.) [28,27]. However, it is still challenging for the effective detection of nuclei in histopathological

images since we usually observe large amounts of variations in appearance and arrangement of nuclei across different samples [25,7].

Recently, since deep learning (DL) has shown excessively success in the field of computer vision on various natural image detection tasks [13,4], many researchers set out to develop DL algorithms to address the above challenges on nucleus detection tasks [21,11,26]. However, training an accurate and reliable DL model requires amounts of labeled data that will increase the annotation burden for pathologists [22,24,23]. In order to reduce the labeling costs, several active learning (AL) based object detection algorithms have been proposed aiming at querying the most valuable samples for annotation [17]. For instance, Kao *et al.* [9] design a novel query criterion by considering the measurements of localization tightness and localization stability. Yoo *et al.* [29] propose a simple but efficient AL method with the loss prediction module for the object detection task. All these studies indicate that the AL learning paradigm can effectively reduce the annotation efforts for experts.

Although much progress has been achieved, the existing AL based object detection studies usually work on the closed-set assumption where the labeled and unlabeled data are with the same class distribution. In real-word applications, the unlabeled pool usually contains the non-target samples from the unknown classes [15]. For example, suppose that our target is to detect tumor, lymphocytes and stromal nuclei from the pathological image patches. However, many unknown class nuclei (e.g., plasma, macrophages) are also involved in the unlabeled pool and labeling these non-target nuclei will waste the annotation efforts from the experts. We call this scenario in which the unlabeled data comes from both known and unknown classes as an open-set annotation problem [2]. To the best of our knowledge, only two studies consider such an AL scenario. Specifically, Ning *et al.* [15] propose the first AL algorithm (i.e., LfOSA) for open-set annotation that can dynamically select the examples with highest probability from known classes for target model training. Based on LfOSA, Qu *et al.* [16] further query the most valuable samples from the target classes for annotation. However, both of these two studies focus on the classification tasks, an effective and practical AL system for the nucleus detection task is highly desired since the tumor micro-environment revealed by pathological images is consisted of many kinds of cell types, and a deployed nucleus detection system will have high chance to face the unknown conditions.

Based on the above consideration, we propose a novel AL framework called OSAL-ND(**O**pen-**S**et **A**ctive **L**earning for **N**ucleus **D**etection) for nucleus detection under the open-set scenario. Specifically, in the first stage of OSAL-ND, a prototype-based query strategy based on the auxiliary detector is used to select a candidate set from known classes as pure as possible. In the second stage of OSAL-ND, we develop the target detector and query the most informative samples from the candidate set for annotation. Experiments are conducted on the NuCLS dataset with different number of unknown classes. The experimental results demonstrate that the proposed approach can significantly improve the

selection quality of known classes and achieve higher detection accuracy with lower annotation burden than the existing studies.

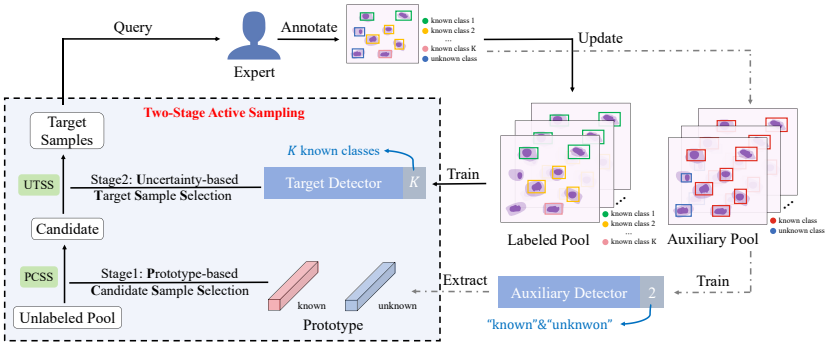

Fig. 1. Flowchart of OSAL-ND. In the first stage, we develop a prototype-based candidate sample selection (PCSS) strategy to select a candidate set from known classes as pure as possible based on the auxiliary detector. Then, based on the target detector, an uncertainty-based target sample selection (UTSS) strategy is designed to select target samples from the candidate set that are most valuable for the nucleus detection task. The auxiliary and target detectors will be updated after the target samples are annotated and incorporated for model training in each round of AL.

2 Method

2.1 Problem Formulation

In the open-set environment for nucleus detection, we define a set of classes denoted as $\mathcal{C} = \mathcal{C}_{kno} \cup \mathcal{C}_{unk}$, where $\mathcal{C}_{kno} = \{c_k\}_{k=1}^{K}$ and $\mathcal{C}_{unk} = \{c_s\}_{s=1}^{S}$ represent the set of K known and S unknown classes, respectively. Suppose that we have a labeled pool $\mathcal{L} = \{x_i^L\}_{i=1}^{n^L}$ with n^L samples, where the nuclei in each x_i^L belong to one of the known classes $\mathcal{C}_{kno}$. The unlabeled pool $\mathcal{U} = \{x_j^U\}_{j=1}^{n^U}$ contains n^U samples, whose nucleus category information comes from both known and unknown classes (i.e., $\mathcal{C}_{kno} \cup \mathcal{C}_{unk}$). The goal of our OSAL-ND is to query valuable samples from the unlabeled pool that can help improve the nucleus detection performance on the known classes, while avoiding to annotating samples whose included objects are mostly come from unknown classes that will lead to a waste of annotation budget.

2.2 Flowchart of the Proposed OSAL-ND

Fig. 1 shows the flowchart of our two-stage OSAL-ND. In the first stage of OSAL-ND, we present a prototype-based candidate sample selection (PCSS) strategy

to select a candidate set including samples from the unlabeled data that are far away from the unknown classes. Then, we further propose an uncertainty-based target sample selection (UTSS) method to select the most valuable samples from the candidate set for the detection task on the known classes. After all the target samples are annotated by the experts, the detection model will be updated for the next round of AL.

2.3 Prototype-based Candidate Sample Selection (PCSS)

In PCSS, we introduce an auxiliary labeled pool $\mathcal{A} = \{x_l^A\}_{l=1}^{N_A}$ consisted of N_A samples, where the nuclei in each sample are annotated with "known" or "unknown". In order to reject the unknown nuclei for annotation, we apply the prototypical representation learning to generate the prototypes of both "known" and "unknown" classes (i.e., p_{kno}, p_{unk}) for candidate sample selection. Specifically, based on the auxiliary pool, we firstly design an auxiliary detector by the aid of Faster R-CNN [18] with a ResNet-50 backbone to detect and distinguish the "known" and "unknown" class nuclei. In addition to the regression and classification loss in Faster R-CNN, we incorporate a prototype learning loss. Mathematically, let $f_c^t \in \mathbb{R}^d$ be the feature vector of the *t-th* nucleus generated by the RoI head of the auxiliary detector with category $c \in \{kno, unk\}$. Then, the prototype loss for the *t-th* nucleus can be defined as:

$$L(f_c^t) = l(f_c^t, p_{kno}) + l(f_c^t, p_{unk}) \tag{1}$$

where

$$l(f_c^t, p_a) = \begin{cases} D(f_c^t, p_a), & c = a \\ \max\{0, \Delta - D(f_c^t, p_a)\}, & \text{otherwise} \end{cases} \tag{2}$$

Here, $D(f_c^t, p_a)$ calculates the Euclidean distance between f_c^t and p_a, Δ is a margin variable and we set $\Delta = 10$ in this study. As shown in Eqs. 1 and 2, the prototype loss aims at learning the prototypes that are the representative embeddings of the "known" and "unknown" classes, respectively. Meanwhile, it also encourages the larger distance between the learned prototypes of "known" and "unknown" classes. In each round of AL, we firstly sum up the prototype loss for all nuclei in the auxiliary labeled pool to update the prototype $\{p_{kno}, p_{unk}\}$. Then, for each image in the unlabeled pool, we count the number of known class nuclei whose features generated by the RoI head is closer to p_{kno} than p_{unk}. Finally, we select the top $2N$ images from the unlabeled pool with the highest number of known class nuclei and then feed them into the candidate set.

2.4 Uncertainty-based Target Sample Selection (UTSS)

Considering the image with rich information is crucial for increasing the generalization ability of the detection model [12], we further develop an uncertainty-based target sample selection (UTSS) strategy to query the most uncertainty samples from the candidate set for the detection task on the known classes.

Since the object-detection problem can be considered as the combination of the object-classification and object-localization tasks, we consider both of these two sides to calculate the uncertainty information of the j-th sample in the unlabeled pool (i.e., I_j) as:

$$I_j = CI_j \cdot LI_j \tag{3}$$

where CI_j and LI_j refer to the uncertainty information for the object-classification and object-localization tasks, respectively.

On one hand, we adopt an evidence-based uncertainty estimation technique proposed in [6] to calculate CI_j since the traditional entropy based methods tend to produce inflated confidence values even for the incorrect predictions [14]. More specifically, for the unlabeled images x_j^U with B bounding boxes, suppose that the current target model can predict the label of each bounding box from K known classes by a K-dimensional vector $h^b \in R^K$ $(b = 1, 2, ..., B)$. Then, we follow the study in [3] applying the ReLU activation function on h^b to derive the evidence vector, i.e., $E^b = relu(h^b) = [e_1^b, e_2^b, ..., e_K^b] \in R^K$. Next, we use subjective logic [8] for the connection of the evidence vector to the parameters of Dirichlet distribution, and the Dirichlet strength is defined as $Q^b = \sum_{k=1}^{K}(e_k^b+1)$, by which we can assign a belief mass $q_k^b = e_k^b/Q^b$ for each class k. Intuitively, more evidence for a class leads to a higher belief mass assigned to it and thus the classification uncertainty for the b-th bounding box can be formulated by:

$$Un^b = 1 - \sum_{k=1}^{K} q_k^b \tag{4}$$

Finally, the uncertainty of x_j^U in the classification branch (i.e., CI_j) can be calculated by averaging the uncertainty of all its involved bounding boxes as:

$$CI_j = \frac{1}{B}\sum_{b=1}^{B} Un^b \tag{5}$$

On the other hand, we consider the localization uncertainty of an image based on the localization tightness of the bounding boxes. Here, the localization tightness measures how tight a predicted bounding box can enclose the proposal and we apply the index of IoU to define it. Obviously, the localization uncertainty of a bounding box is high if its localization tightness is low, indicating that our model is less confident on it. Specifically, given x_j^U with B bounding boxes predicted by the target model, we define the b-th bounding box and its corresponding proposal as box^b and $prop^b$, respectively. Then, the localization uncertainty (i.e., LI_j) can be calculated by averaging the uncertainty for all its bounding boxes defined below:

$$LI_j = \frac{1}{B}\sum_{b=1}^{B}(1 - \frac{box^b \cap prop^b}{box^b \cup prop^b}) \tag{6}$$

Table 1. The open-set learning environment for nucleus detection.

Unknown Settings	Known Classes	Unknown Classes
5 known + 2 unknown	Tum, Lym, Str, Pla, Mit	Mac, Oth
4 known + 3 unknown	Tum, Lym, Str, Pla	Mit, Mac, Oth
3 known + 4 unknown	Tum, Lym, Str	Pla, Mit, Mac, Oth

To select the most uncertain N samples from the candidate set introduced in Section 2.3, we hope the classification uncertainty (shown in Eq. 5) and the localization uncertainty (shown in Eq. 6) to be large at the same time, and such criteria is indicated in Eq. 3.

3 Experiments

Dataset and Settings To validate the effectiveness of the proposed approach, we perform experiments on the NuCLS dataset [1] that is consisted of nuclei with 7 categories including tumor (Tum, 6658 nuclei), lymphoc (Lym, 1726 nuclei), stromal (Str, 1970 nuclei), plasma_cell (Pla, 1075 nuclei), mitotic_figure (Mit, 49 nuclei), macrophage (Mac, 183 nuclei), and other (Oth, 119 nuclei). To construct the open-set learning environment, we set the number of unknown classes as 2, 3 and 4 for all experiments, and more details can be found in Table 1. For OSAL-ND and all the compared AL methods, we randomly divide the dataset into five folds, with four folds used for model training and the remaining for performance evaluation on the target detector. In the train set, we randomly select 5% samples as initialization labeled set $\mathcal{L}$, while the remaining samples are designated as the unlabeled pool $\mathcal{U}$. For each round of AL, we set the number of samples (i.e., N) required annotation as 15% of the training set.

Baselines and Metric We compare our OSAL-ND with the following 7 baseline methods: *i*) **Random**: Query samples randomly. *ii*) **Uncertainty** [10,12]: Query samples with the largest uncertainty of predictions. *iii*) **Coreset** [20]: Query representative samples with diversity. *iv*) **LAAL** [9]: Query localization-aware samples with the highest tightness and stability. *v*) **LL4AL** [29]: Query samples based on the learning loss. *vi*) **CALD** [30]: Query samples based on the consistency. *vii*) **LfOSA** [15]: a one-stage framework for open-set AL. *viii*) **OpenAL** [16]: a two-stage framework for open-set AL. Among these methods, only LfOSA and OpenAL are designed for open-set AL. However, both of these two methods are designed for the classification task, and we combine it with our proposed localization uncertainty introduced in Eq. 6 to implement the AL for object detection. We evaluate the performance of our method and its competitors by the measurement of mAP at an IoU threshold of 0.5.

Comparisons of nucleus detection performance with different number of unknown classes In Fig. 2, we plot the mAP curves with the proportion of

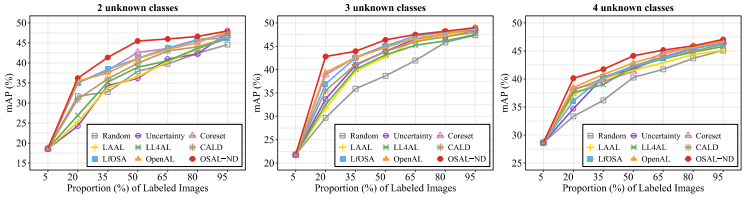

Fig. 2. Comparisons of nucleus detection performance on NuCLS with 2 (first column), 3 (second column), and 4 (third column) unknown classes.

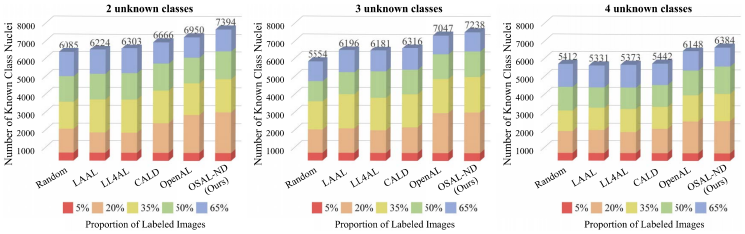

Fig. 3. Comparison of the number of queried nuclei from known classes with different proportions of labeled images.

labeled images increasing for different number of unknown classes. It is obviously that the proposed OSAL-ND consistently outperforms other methods regardless of the number of unknown classes set in the open-set learning scenario. Specifically, in comparison with the traditional AL algorithms applied in the closed-set scenario for object detection (i.e., Random, Uncertainty, Coreset, LAAL, LL4AL and CALD), our OSAL-ND can always achieve higher mAP values since we consider the presence of unknown classes in the open-set scenario. Moreover, we also find that our method is superior to the two open-set AL algorithms(i.e., LfOSA and OpenAL). This is because LfOSA only focuses on querying samples from known classes for annotation, which overlooks the importance of labeling the uncertainty samples for improving the detection performance of the model. On the other hand, although OpenAL selects the most informative samples for annotation, it is calculated via the measurement of entropy that may produce inflated confidence values even for the incorrect predictions [14].

Comparisons of different methods for querying nuclei from known classes In Fig. 3, we compare the number of queried nuclei from known classes among different methods. It is evident that OSAL-ND can more effectively identify nuclei from known classes. This is because our OSAL-ND selects known class nuclei based on the prototype learning, which can more accurately characterize the difference between known and unknown class samples.

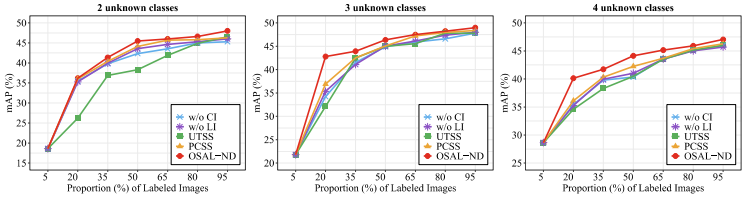

Fig. 4. Ablation study on NuCLS with 2 (first column), 3 (second column), and 4 (third column) unknown classes.

Ablation Study To further evaluate the effectiveness of our method, we compare OSAL-ND with its following variants. **w/o CI**: Select target samples without considering the uncertainty information for the object-classification task. **w/o LI** : Select target samples without considering the uncertainty information for the object-localization task. **UTSS**: Only applying the uncertainty-based target sample selection strategy for AL. **PCSS**:Only applying the prototype-based candidate sample selection strategy for AL. As shown in Fig. 4, the proposed OSAL-ND is superior to **w/o CI** and **w/o LI**, indicating that the uncertainty information is important for both object localization and classification tasks. In addition, it is obvious that OSAL-ND can achieve higher mAP than UTSS and PCSS with different proportions of labeled data, indicating the advantage of our method that considers both purity and uncertainty information in the sample selection process.

Comparisons of visualization results among different methods Fig. 5 presents the sample visualization results of different methods using 20% labeled data. On one hand, OSAL-ND shows its superior performance in distinguishing different nucleus types. We can clearly find that LfOSA and OpenAL are more likely to misclassify nucleus category in comparison with our OSAL-ND. On the other hand, OSAL-ND outperforms LfOSA and OpenAL in terms of the localization task. Specifically, LfOSA and OpenAL exhibit issues with higher missing detection rate (shown with $\otimes$ symbol) in comparison with OSAL-ND. Moreover, OpenAL also faces the problems of over-detection (shown with arrow symbol) when comparing with OSAL-ND.

4 Conclusion

In this paper, we propose OSAL-ND as a novel AL framework for detecting nuclei in the open-set environment. OSAL-ND is a two-stage AL framework that can effectively reduce the annotation burden for pathologists. In the first stage, we select a candidate set as pure as possible. In the second stage, we consider both classification and localization uncertainty to select the most informative samples for annotation. The experimental results demonstrate the superior performance of our OSAL-ND in comparison with the existing studies.

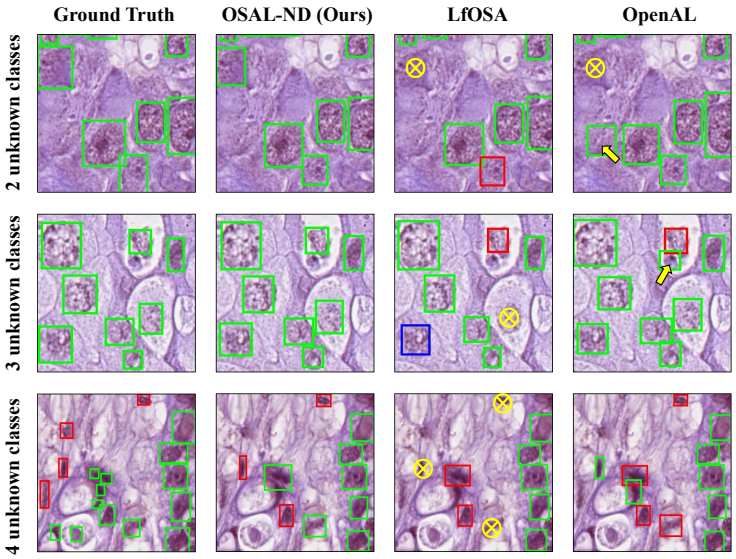

Fig. 5. Comparison of visualization results among different methods.

Acknowledgments. This work was supported by the National Natural Science Foundation of China (Nos. 62136004, 62272226, 62102188), Key Research and Development Plan of Jiangsu Province, China under Grant BE2022842, Postdoctoral Fellowship Program of CPSF (No. GZC20242233).

Disclosure of Interests. The authors have no competing interests to declare that are relevant to the content of this article.

References

1. Amgad, M., Atteya, L.A., Hussein, H., Mohammed, K.H., Hafiz, E., Elsebaie, M.A., Alhusseiny, A.M., AlMoslemany, M.A., Elmatboly, A.M., Pappalardo, P.A., et al.: Nucls: A scalable crowdsourcing approach and dataset for nucleus classification and segmentation in breast cancer. GigaScience **11** (2022)
2. Geng, C., Huang, S.j., Chen, S.: Recent advances in open set recognition: A survey. IEEE Transactions on Pattern Analysis and Machine Intelligence **43**(10), 3614–3631 (2020)
3. Glorot, X., Bordes, A., Bengio, Y.: Deep sparse rectifier neural networks. In: Proceedings of the Fourteenth International Conference on Artificial Intelligence and Statistics. pp. 315–323. JMLR Workshop and Conference Proceedings (2011)
4. Guo, X., Liu, X., Ren, Z., Grosz, S., Masi, I., Liu, X.: Hierarchical fine-grained image forgery detection and localization. In: Proceedings of the IEEE/CVF Conference on Computer Vision and Pattern Recognition. pp. 3155–3165 (2023)
5. Gurcan, M.N., Boucheron, L.E., Can, A., Madabhushi, A., Rajpoot, N.M., Yener, B.: Histopathological image analysis: A review. IEEE Reviews in Biomedical Engineering **2**, 147–171 (2009)

6. Han, Z., Zhang, C., Fu, H., Zhou, J.T.: Trusted multi-view classification. arXiv preprint arXiv:2102.02051 (2021)
7. Huang, J., Li, H., Sun, W., Wan, X., Li, G.: Prompt-based grouping transformer for nucleus detection and classification. In: International Conference on Medical Image Computing and Computer-Assisted Intervention. pp. 569–579. Springer (2023)
8. Jsang, A.: Subjective Logic: A formalism for reasoning under uncertainty. Springer Publishing Company, Incorporated (2018)
9. Kao, C.C., Lee, T.Y., Sen, P., Liu, M.Y.: Localization-aware active learning for object detection. In: Computer Vision–ACCV 2018: 14th Asian Conference on Computer Vision, Perth, Australia, December 2–6, 2018, Revised Selected Papers, Part VI 14. pp. 506–522. Springer (2019)
10. Lewis, D.D.: A sequential algorithm for training text classifiers: Corrigendum and additional data. In: Acm Sigir Forum. vol. 29, pp. 13–19. ACM New York, NY, USA (1995)
11. Litjens, G., Kooi, T., Bejnordi, B.E., Setio, A.A.A., Ciompi, F., Ghafoorian, M., Van Der Laak, J.A., Van Ginneken, B., Sánchez, C.I.: A survey on deep learning in medical image analysis. Medical Image Analysis **42**, 60–88 (2017)
12. Luo, W., Schwing, A., Urtasun, R.: Latent structured active learning. Advances in Neural Information Processing Systems **26** (2013)
13. Mahmoud, A., Hu, J.S., Waslander, S.L.: Dense voxel fusion for 3d object detection. In: Proceedings of the IEEE/CVF Winter Conference on Applications of Computer Vision. pp. 663–672 (2023)
14. Moon, J., Kim, J., Shin, Y., Hwang, S.: Confidence-aware learning for deep neural networks. In: International Conference on Machine Learning. pp. 7034–7044. PMLR (2020)
15. Ning, K.P., Zhao, X., Li, Y., Huang, S.J.: Active learning for open-set annotation. In: Proceedings of the IEEE/CVF Conference on Computer Vision and Pattern Recognition. pp. 41–49 (2022)
16. Qu, L., Ma, Y., Yang, Z., Wang, M., Song, Z.: Openal: An efficient deep active learning framework for open-set pathology image classification. In: International Conference on Medical Image Computing and Computer-Assisted Intervention. pp. 3–13. Springer (2023)
17. Ren, P., Xiao, Y., Chang, X., Huang, P.Y., Li, Z., Gupta, B.B., Chen, X., Wang, X.: A survey of deep active learning. ACM Computing Surveys (CSUR) **54**(9), 1–40 (2021)
18. Ren, S., He, K., Girshick, R., Sun, J.: Faster r-cnn: Towards real-time object detection with region proposal networks. Advances in Neural Information Processing Systems **28** (2015)
19. Roy, S., kumar Jain, A., Lal, S., Kini, J.: A study about color normalization methods for histopathology images. Micron **114**, 42–61 (2018)
20. Sener, O., Savarese, S.: Active learning for convolutional neural networks: A core-set approach. International Conference on Learning Representations (2018)
21. Shen, D., Wu, G., Suk, H.I.: Deep learning in medical image analysis. Annual Review of Biomedical Engineering **19**, 221–248 (2017)
22. Singla, A., Bertino, E., Verma, D.: Overcoming the lack of labeled data: Training intrusion detection models using transfer learning. In: 2019 IEEE International Conference on Smart Computing (SMARTCOMP). pp. 69–74. IEEE (2019)
23. Srinidhi, C.L., Ciga, O., Martel, A.L.: Deep neural network models for computational histopathology: A survey. Medical Image Analysis **67**, 101813 (2021)

24. Tang, Y.P., Wei, X.S., Zhao, B., Huang, S.J.: Qbox: Partial transfer learning with active querying for object detection. IEEE Transactions on Neural Networks and Learning Systems (2021)
25. Tofighi, M., Guo, T., Vanamala, J.K., Monga, V.: Prior information guided regularized deep learning for cell nucleus detection. IEEE Transactions on Medical Imaging **38**(9), 2047–2058 (2019)
26. Xie, Y., Xing, F., Shi, X., Kong, X., Su, H., Yang, L.: Efficient and robust cell detection: A structured regression approach. Medical Image Analysis **44**, 245–254 (2018)
27. Xing, F., Xie, Y., Shi, X., Chen, P., Zhang, Z., Yang, L.: Towards pixel-to-pixel deep nucleus detection in microscopy images. BMC bioinformatics **20**(1), 1–16 (2019)
28. Xing, F., Yang, L.: Robust nucleus/cell detection and segmentation in digital pathology and microscopy images: a comprehensive review. IEEE Reviews in Biomedical Engineering **9**, 234–263 (2016)
29. Yoo, D., Kweon, I.S.: Learning loss for active learning. In: Proceedings of the IEEE/CVF Conference on Computer Vision and Pattern Recognition. pp. 93–102 (2019)
30. Yu, W., Zhu, S., Yang, T., Chen, C.: Consistency-based active learning for object detection. In: Proceedings of the IEEE/CVF Conference on Computer Vision and Pattern Recognition. pp. 3951–3960 (2022)